MOLECULAR AND CELLULAR BIOLOGY, Aug. 1994, p. 5182–5191
0270-7306/94/$04.00+0

Vol. 14, No. 8

p53 Domains: Structure, Oligomerization, and Transformation

PIN WANG, MICHAEL REED, YUN WANG, GREGORY MAYR, JUDITH E. STENGER, MARY E. ANDERSON, JOHN F. SCHWEDES, AND PETER TEGTMEYER*

Department of Molecular Genetics and Microbiology, State University of New York, Stony Brook, New York 11794

Received 28 March 1994/Returned for modification 6 May 1994/Accepted 19 May 1994

Wild-type p53 forms tetramers and multiples of tetramers. Friedman et al. (P. N. Friedman, X. B. Chen, J. Bargonetti, and C. Prives, Proc. Natl. Acad. Sci. USA 90:3319–3323, 1993) have reported that human p53 behaves as a larger molecule during gel filtration than it does during sucrose gradient sedimentation. These differences argue that wild-type p53 has a nonglobular shape. To identify structural and oligomerization domains in p53, we have investigated the physical properties of purified segments of p53. The central, specific DNA-binding domain within murine amino acids 80 to 320 and human amino acids 83 to 323 behaves predominantly as monomers during analysis by sedimentation, gel filtration, and gel electrophoresis. This consistent behavior argues that the central region of p53 is globular in shape. Under appropriate conditions, however, this segment can form transient oligomers without apparent preference for a single oligomeric structure. This region does not enhance transformation by other oncogenes. The biological implications of transient oligomerization by this central segment, therefore, remain to be demonstrated. Like wild-type p53, the C terminus, consisting of murine amino acids 280 to 390 and human amino acids 283 to 393, behaves anomalously during gel filtration and apparently has a nonglobular shape. Within this region, murine amino acids 315 to 350 and human amino acids 323 to 355 are sufficient for assembly of stable tetramers. The finding that murine amino acids 315 to 360 enhance transformation by other oncogenes strongly supports the role of p53 tetramerization in oncogenesis. Amino acids 330 to 390 of murine p53 and amino acids 340 to 393 of human p53, which have been implicated by Sturzbecher et al. in tetramerization (H.-W. Sturzbecher, R. Brain, C. Addison, K. Rudge, M. Remm, M. Grimaldi, E. Keenan, and J. R. Jenkins, Oncogene 7:1513–1523, 1992), do not form stable tetramers under our conditions. Our findings indicate that p53 has at least two autonomous oligomerization domains: a strong tetramerization domain in its C-terminal region and a weaker oligomerization domain in the central DNA binding region of p53. Together, these domains account for the formation of tetramers and multiples of tetramers by wild-type p53. The tetramerization domain is the major determinant of the dominant negative phenotype leading to transformation by mutant p53s.

Many human cancers are associated with a loss of p53 function (14, 17). This correlation argues that wild-type (WT) p53 suppresses cellular proliferation and tumor formation. Indeed, in experimental systems, the expression of WT p53 suppresses transformation by other oncogenes (4, 7, 13). In contrast, many mutant p53s enhance transformation under the same conditions. These findings argue that mutant p53 interferes with the suppression functions of endogenous WT p53. Because p53 forms oligomeric structures, the dominant negative phenotype of the mutants has been attributed to the formation of mixed WT and mutant oligomers (12). In support of this hypothesis, the C-terminal region of p53 has both oligomerization and transformation functions (18, 22, 23, 28). The oligomerization domains of p53, however, have not been mapped in detail.

Although the suppression functions of p53 are not completely understood, one mechanism by which p53 acts is the direct activation of transcription via site-specific DNA binding (5, 9, 15). Presumably, p53 activates genes that inhibit cellular proliferation such as the *WAF1* (*Cip1*) gene (3, 6, 11). The role of p53 oligomerization in DNA binding and transactivation is not clear. Recently, we and others showed that p53 has two autonomous DNA-binding regions (1, 20, 26, 29). One domain, from amino acids 280 to 390 (segment 280–390), forms stable tetramers and binds DNA nonspecifically. The biological significance, if any, of this DNA binding activity remains to be determined. A second domain, from amino acids 80 to 290 (segment 80–290), does not form stable tetramers but binds DNA specifically. Furthermore, amino acids 1 to 290, which include both the specific DNA-binding domain and the N-terminal acidic region, activate a p53-specific promoter in vivo. The specific DNA binding and transactivating functions of p53, therefore, do not require stable tetramerization. Because the DNA recognition site for p53 consists of four imperfect repeats, however, it would be surprising if oligomerization did not contribute to the DNA binding function of p53.

We have undertaken the present study to define further the oligomerization properties of p53 and the role of oligomerization in cellular transformation. There has been some disagreement about the nature of the various quaternary structures formed by p53. This confusion is the result of a number of factors. First, purified p53 consists of many oligomeric forms that require high-resolution techniques for analysis. Second, p53 appears to have an unusual shape that leads to anomalous behavior during gel filtration (8). Finally, murine and human p53s have been studied independently but have not been directly compared. We have, therefore, used a variety of techniques to define the quaternary structures of murine and human p53s. The availability of purified segments of p53 has allowed us to separate two autonomous oligomerization domains of the protein. We find that murine amino acids 315 to 350 and human amino acids 323 to 355 encode a strong tetramerization domain. Murine amino acids 80 to 320 and human amino acids 83 to 323 form unstable oligomers without a preferred species. We also present evidence that the C terminus of p53 is a major determinant of its nonglobular

* Corresponding author.

shape. In contrast, the central conserved region behaves as a globular protein during sedimentation and gel filtration.

MATERIALS AND METHODS

Expression plasmids. We have previously described plasmids used for expression of WT p53 or segments of p53. The pIT plasmid was designed for recombination with baculovirus vectors and overexpression of p53 in insect cells (22). The pBT plasmid utilizes an inducible T7 promoter for transient overexpression of p53 in bacteria (29). The pCMH6K plasmid includes the immediate-early promoter of cytomegalovirus for strong expression of p53 in animal cells (29). These plasmids express WT p53 or segments of p53 with a 22-amino-acid N-terminal tag that encodes six histidines for purification by metal affinity chromatography and a hemagglutinin epitope for identification with monoclonal antibodies. To exclude the possibility of mutations within p53 segments, we isolated and tested two independent clones expressing each p53 segment. Plasmids were purified by CsCl centrifugation.

Overexpression and metal affinity purification of p53. Because WT p53 is mostly insoluble when produced in bacteria, we overexpressed WT p53 by infecting insect cells with baculovirus expression vectors and purified p53 as previously described (29). In brief, p53 was extracted from SF9 cells in lysis buffer (50 mM Tris-HCl [pH 9.0], 150 mM NaCl, 0.1% Nonidet P-40, 10% glycerol, 1 mM phenylmethylsulfonyl fluoride, 50 μg of aprotinin per ml, 50 μg of leupeptin per ml, 10 μg of pepstatin A per ml, 1 mM benzamidine, 5 mM β-mercaptoethanol), clarified by centrifugation, and bound to Ni-nitrilotriacetic acid (NTA)-agarose (Qiagen, Inc.) at 4°C. After being washed extensively with lysis buffer (pH 7.0), Ni-NTA-agarose was eluted with lysis buffer (pH 7.0) containing increasing concentrations of imidazole (25, 50, 100, and 250 mM). p53-containing fractions were dialyzed overnight at 4°C against 20 mM Tris-HCl (pH 8.0)–100 mM NaCl–50% glycerol (dialysis buffer) and stored in aliquots at −70°C.

All p53 segments were overexpressed in bacteria (HMS174 or BL21) as previously described (29). In brief, bacteria transformed by pBT plasmids were expanded from a single colony to a 500-ml culture in two steps, and cells were induced with IPTG (isopropyl-β-D-thiogalactopyranoside) at a final concentration of 1 mM and incubated for 4 h at 30°C. Cells were suspended in lysis buffer and broken with a French press at 1,500 lb/in^2. Lysates were cleared by centrifugation and bound to Ni-NTA-agarose in a small column. The bound p53 was washed, eluted, dialyzed, and stored as described above.

SDS-PAGE. Purified proteins were separated by 15% polyacrylamide gel electrophoresis (PAGE) in the presence of sodium dodecyl sulfate (SDS) as described by Laemmli and stained with Coomassie blue (16). Aliquots of the same p53 preparations were used for analysis of quaternary structure by sucrose gradient analysis, gel filtration, and protein cross-linking in conjunction with SDS-PAGE (see below).

Sucrose gradient analysis of p53 oligomers. A mixture (in 0.14 ml) of purified WT p53 and fragments of p53 (10 μg each) was layered on a 4-ml linear 5 to 20% (wt/wt) sucrose density gradient in 50 mM Tris-HCl (pH 7.0)–150 mM NaCl–50 mM imidazole–10% glycerol–1 mM dithiothreitol. The gradient was centrifuged for 20 h at 50,000 rpm in a Beckman SW60 rotor at 5°C. Fractions of approximately 0.2 ml were collected from the bottom of the gradient, precipitated with 10% trichloroacetic acid in the presence of 20 μg of bovine serum albumin as a carrier, and analyzed by SDS–15% PAGE. Molecular weight markers were analyzed in a parallel gradient under the same conditions.

Gel filtration of p53 oligomers. A mixture (in 0.5 ml) of purified WT p53 samples and segments of p53 (10 to 40 μg each) was fractionated by gel filtration through a Superose 12 HR column (10 by 300 mm; Pharmacia) equilibrated with 50 mM Tris-HCl (pH 7.0)–150 mM NaCl–50 mM imidazole–10% glycerol–0.01% sodium azide. The column was run with a Pharmacia fast protein liquid chromatography system at 30 ml/h at 5°C. Fractions (0.2 ml each) were collected, trichloroacetic acid precipitated, and analyzed by SDS–15% PAGE. Molecular weight protein standards were analyzed under the same conditions.

Gradient gel electrophoresis of cross-linked oligomers of p53. The quaternary structures of p53 segments were analyzed by protein cross-linking in conjunction with SDS gradient gel electrophoresis as previously described (27). Purified p53 segments (2 μg each) were incubated for 30 min at 30°C in 30 μl of the same buffer used for sedimentation and gel filtration. Increasing concentrations of freshly diluted glutaraldehyde (Sigma) were added as indicated in the figures. Products of the cross-linking reactions were analyzed by SDS-PAGE. All of the gel components were those described by Laemmli (16) except that we used an 80:1 ratio of acrylamide to bisacrylamide (pH 8.8) to prevent protein retardation in the stacking gel (empirically determined). Samples were diluted twofold in sample buffer containing 4% (wt/vol) SDS and 5% (vol/vol) β-mercaptoethanol and heated for 5 min at 100°C immediately prior to loading onto the gel. Samples were electrophoresed through 4 to 20% or 8 to 20% polyacrylamide gels in 0.1% SDS at 200 V for 4 h at room temperature. Following electrophoresis, gels were silver stained (19).

Suppression and transformation assays. We previously described a combined assay for suppression and enhancement of transformation (22). In brief, fourth-passage rat embryo fibroblasts (REF) were grown to subconfluency in 10-cm-diameter Falcon plates in Dulbecco modified Eagle medium with 10% fetal bovine serum and antibiotics. DOTAP (Boehringer Mannheim) was used to triply transfect REF cells with 2.5 μg of pSP72-RAS (expressing activated *ras*), 2.5 μg of pBS-E1A (expressing adenovirus E1A), and 5.0 μg of pCMH6K DNA with or without a *p53* insert. Cells were incubated at 37°C in a moist CO_2 incubator and fed with Dulbecco modified Eagle medium and 10% fetal bovine serum every 3 to 4 days. After 12 days, cells were washed twice with phosphate-buffered saline, fixed with methanol for 5 min, and stained with 0.05% Coomassie blue in 50% methanol–10% acetic acid for 1 h. Plates were washed with water and air dried, and transformed foci were counted.

Immunoprecipitation and immunoblotting. REF cells in two 10-cm-diameter plates were transfected with 20 μg of pCMH6K plasmid DNAs expressing WT p53 or segments of p53 by calcium phosphate precipitation (2). After 40 h, cells were washed with phosphate-buffered saline, and p53 was extracted with 0.5 ml of lysis buffer for 30 min on ice. Extracts were clarified by low-speed centrifugation, and tagged p53s were bound to 100 μl of Ni-NTA-agarose overnight at 4°C. After beads were washed twice with 1 ml of lysis buffer, tagged p53s were released with 100 μl of SDS loading buffer for gel electrophoresis. Concentrated and partially purified p53s were analyzed by SDS-PAGE and immunoblotting with a kit for enhanced chemiluminescence (Amersham). We used 600 μg of monoclonal antibody against the hemagglutinin epitope within the N-terminal tag of p53 (12CA5; Babco) in 100 ml of Tris-buffered saline with 5% milk for immunoblotting.

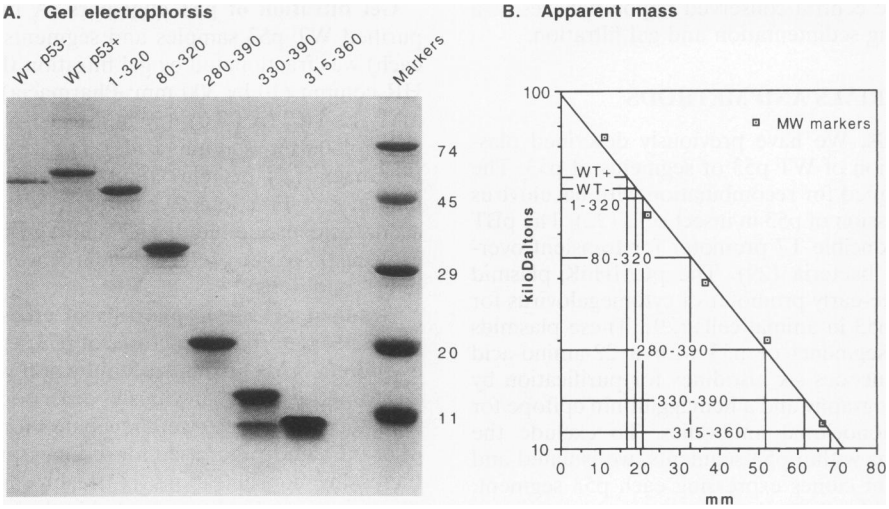

FIG. 1. SDS-PAGE of murine WT p53 and segments of p53. (A) SDS-PAGE and Coomassie blue staining of purified WT p53 without (−) or with (+) 22-amino-acid tags and segments of p53 segments with tags. Molecular mass markers consisting of transferrin (74 kDa), bovine serum albumin (45 kDa), carbonic anhydrase (29 kDa), soybean trypsin inhibitor (20 kDa), and cytochrome *c* (11 kDa) are shown on the right. (B) Molecular mass plot of standard markers. The positions of p53 segments are related to their apparent molecular masses by horizontal and vertical lines.

RESULTS

SDS gel electrophoresis of purified murine WT p53 and segments of p53. We wanted to identify autonomous structural and oligomerization domains in p53 to develop a better understanding of p53 functions. For this purpose, we analyzed the structures of murine p53 segments that were previously used to investigate the DNA binding and transformation functions of p53 (22, 29). p53 segments are identified by their amino acid components, which are numbered by the system of Pennica et al. (21). WT p53 and segments of p53 with 22-amino-acid N-terminal tags containing six histidines were purified by metal affinity chromatography. Because WT p53 produced in bacteria is mostly insoluble, we used soluble WT p53 produced in insect cells for studies of purified WT protein. In contrast, segments of p53 produced in bacteria were soluble and could be easily purified. Figure 1A relates purified p53 segments to standard molecular mass markers after SDS-PAGE and Coomassie blue staining. Figure 1B shows the best fit plot of the standards as a diagonal line relating the log of the molecular mass to gel migration for each standard. The vertical and horizontal lines relate the gel migrations of WT p53 and segments of p53 to their apparent molecular masses. Table 1 summarizes these results and compares them with other analyses. Tagged WT p53 and segment 1–320 had apparent molecular masses 10 to 12 kDa larger than predicted by their amino acid compositions. Because tagged WT p53 was only 3 to 4 kDa larger than untagged p53, the 10 to 12 kDa anomalies were not a result of the histidine tag. In contrast, p53 segments 80–320, 280–390, 330–390, and 315–360 had apparent molecular masses about 3 kDa larger than their calculated masses. Anomalies of this size are frequently associated with histidine tags. These findings argue that the major determinant of the anomalous SDS-PAGE of WT p53, tagged or untagged, resides in the first 80 amino acids of p53. The extra protein fragment migrating ahead of segment 330–390 appears to be a proteolytic fragment.

Sucrose gradient sedimentation of murine p53. We used sedimentation through sucrose gradients to study the quaternary structures of purified p53 segments. Mixtures of molecular mass markers (Fig. 2A) and of p53 segments (Fig. 2B) were layered onto two identical 5 to 20% sucrose gradients and centrifuged in parallel as described in Materials and Methods. Gradient fractions were acid precipitated after the addition of carrier bovine serum albumin and were analyzed by SDS-PAGE. Figure 2C shows a diagonal plot of apparent molecular masses as determined by the sedimentation of the markers. Aldolase is a tetramer (161 kDa) while transferrin (74 kDa), ovalbumin (45 kDa), carbonic anhydrase (29 kDa), and cytochrome *c* (11 kDa) are monomers in their native conformations. The vertical and horizontal lines relate the sedimentation of WT p53 and segments of p53 to their apparent molecular masses. WT p53 sediments at the position of aldolase (161 kDa). This result is in good agreement with the sedimentation of human WT p53 reported by Friedman et al. with similar markers (8). Segments 1–320, 80–320, and 330–390 sedimented at positions most consistent with the masses of their monomeric forms (Table 1). Segments 280–390 and 315–360 sedimented ahead of the larger p53 segments 1–320 and 330–390, respectively. This sedimentation profile strongly suggests that the C-terminal segments 280–390 and 315–360 form stable oligomeric forms (Table 1). Nevertheless, the limited resolution of the standard markers and the possibility

TABLE 1. Comparison of apparent molecular masses of p53 determined by different methods

p53 segment	Apparent mass (kDa)			
	Sequence	SDS-PAGE	Sedimentation	Gel filtration
WT	43.5, 174[a]	53	ND[b]	ND
WT tagged	45.9, 184	57	160–180	500
1–320	37.9	50	30–40	55
80–320	29.3	33	30–40	30
280–390	15.0, 60	18	40–50	110
330–390	9.3	13	10–20	15
315–360	7.9, 32	11	20–30	40

[a] Monomeric and tetrameric masses by sequence composition.
[b] ND, not done.

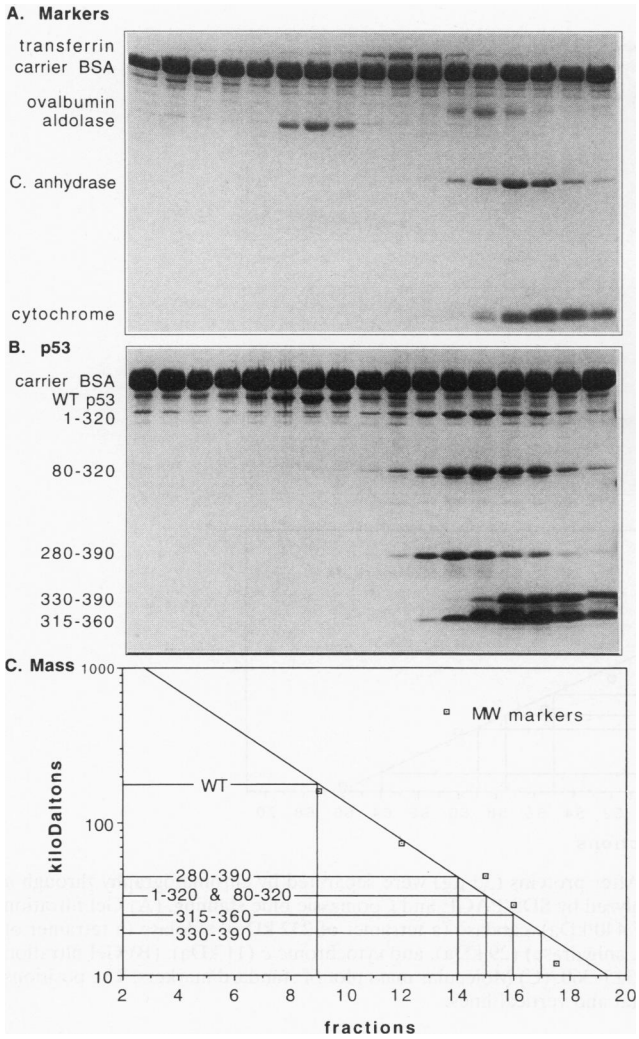

FIG. 2. Sucrose gradient analysis of murine WT p53 and segments of p53. After proteins (10 μg) were centrifuged through 5 to 20% gradients, fractions were concentrated by trichloroacetic acid precipitation in the presence of added bovine serum albumin (carrier BSA) and were analyzed by SDS-PAGE and Coomassie blue staining. (A) Sucrose gradient of a mixture of molecular mass markers: aldolase (a tetramer of 161 kDa), transferrin (74 kDa), ovalbumin (45 kDa), carbonic anhydrase (C. anhydrase) (29 kDa), and cytochrome *c* (11 kDa). (B) Sucrose gradient of a mixture of WT p53 and p53 segments 1–320, 80–320, 280–390, 330–390, and 315–360. (C) Molecular mass plot of standard markers. The positions of p53 segments are related to their apparent molecular masses by horizontal and vertical lines.

of anomalies in p53 shape preclude identification of specific oligomeric structures by sedimentation analysis alone.

Gel filtration of murine p53. Friedman et al. (8) reported that human WT p53 behaves as a larger molecule during gel filtration than it does during sucrose gradient sedimentation. This difference argues that WT p53 has a nonglobular shape. We used a Superose 12 column as described in Materials and Methods to determine the behavior of murine WT p53 and segments of p53 during gel filtration under the same conditions used for the sucrose gradients described above. Analysis of a mixture of molecular weight markers (Fig. 3A) established a standard plot of molecular mass for the column run under standard conditions (the diagonal plot in Fig. 3C). The markers eluted in tight peaks and were well resolved from one another. Furthermore, the markers eluted at the same positions ± one column fraction when reanalyzed under the same conditions (data not shown).

Figure 3B shows the elution profiles of murine WT p53 and segments of p53. The void volume of the column run in Fig. 3B was the same as that of the column shown in Fig. 3A. The vertical and horizontal lines in Fig. 3C relate elution positions to apparent molecular masses, and the results are summarized in Table 1. With the exceptions of segments 1–320 and 80–320, purified p53 segments eluted as symmetrical peaks. Murine WT p53 eluted with an apparent mass of approximately 500 kDa (Table 1); this result is similar to the estimate of Friedman et al. (8). Segment 1–320 behaved as a protein with a mass of 50 to 60 kDa and had an indistinct leading shoulder. This apparent mass is larger than expected on the basis of amino acid content but is similar to the mass established by SDS-PAGE (Table 1). Most of segment 80–320 eluted as a distinct peak of about 30 kDa corresponding closely to its monomeric mass on the basis of either amino acid content or SDS-PAGE. This finding argues that the central conserved region of p53 consists of monomers with globular shapes. This segment, however, also had an indistinct leading shoulder, raising the possibility that it forms weak oligomeric forms that dissociate during gel filtration. Segment 280–390 had an apparent mass of about 110 kDa. As is the case with WT p53, this mass is significantly larger than that expected for a tetramer of segment 280–390. Segment 330–390 had an apparent mass somewhat larger than that established by SDS-PAGE. Finally, most of segment 315–360 eluted at the expected position for a tetramer of that segment. Protein, similar in size to segment 315–360, eluted just behind segment 330–390. Separate analyses of segments 315–360 and 330–390 (data not shown) showed that this peak does not consist of segment 315–360 but rather represents the proteolytic fragment of segment 330–390 seen in the SDS-polyacrylamide gel shown in Fig. 1.

We have repeated these analyses with single p53 segments with or without internal standard markers and have obtained similar results. Behavior of the p53 segments, therefore, reflects neither imperfections in our techniques nor artifactual protein-protein interactions during gel filtration. Our findings relating to WT p53 are in good agreement with those of Friedman et al. (8); molecular mass estimates based on gel filtration data are significantly larger than those based on sedimentation analyses (Table 1). Like WT p53, segment 280–390 demonstrates a larger discrepancy between mass estimates obtained by sedimentation and gel filtration analyses. These findings argue that WT p53 and segment 280–390 have nonglobular shapes. These anomalies complicate analysis of p53 quaternary structure by either sucrose gradients or gel filtration alone. Segment 315–360 had the apparent mass of a tetramer, and segments 1–320, 80–320, and 330–390 behaved predominantly as monomers or somewhat larger in both assays. These findings suggest that each of these segments has an approximately globular shape.

Gradient gel electrophoresis of cross-linked oligomers of murine p53. The quaternary structures of p53 segments were analyzed by protein cross-linking in conjunction with gradient SDS-PAGE. Purified p53 segments (2 μg) were cross-linked with various concentrations of freshly diluted glutaraldehyde and analyzed by gel electrophoresis as described in Materials and Methods. We used the same p53 samples and conditions that were used for sucrose gradient centrifugation and gel filtration.

We previously used chemical cross-linking coupled with gradient SDS-PAGE to show that purified WT murine p53

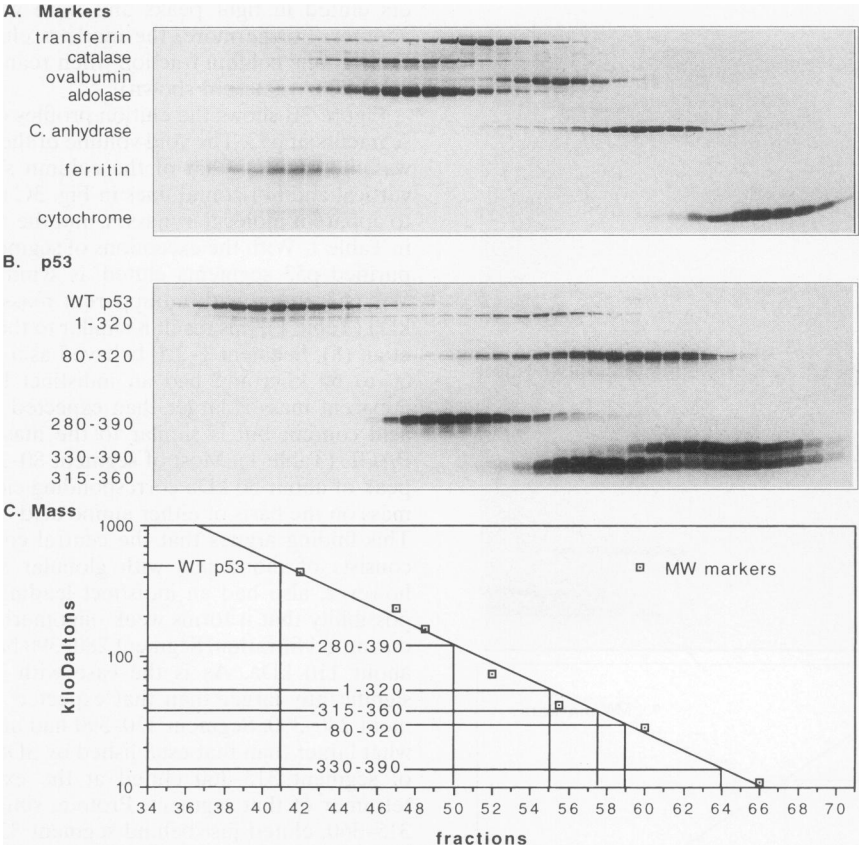

FIG. 3. Gel filtration analysis of murine WT p53 and segments of p53. After proteins (30 μg) were separated by chromatography through a Superose 12 column, fractions were trichloroacetic acid precipitated and analyzed by SDS-PAGE and Coomassie blue staining. (A) Gel filtration of a mixture of molecular mass markers consisting of ferritin (a multimer of 440 kDa), catalase (a tetramer of 232 kDa), aldolase (a tetramer of 161 kDa), transferrin (74 kDa), ovalbumin (43 kDa), carbonic anhydrase (C. anhydrase) (29 kDa), and cytochrome *c* (11 kDa). (B) Gel filtration of a mixture of WT p53 and segments 1–320, 80–320, 280–390, 330–390, and 315–360. (C) Molecular mass plot of standard markers. The positions of p53 segments are related to their apparent molecular masses by horizontal and vertical lines.

forms tetramers and multiples of tetramers (27). Figure 4 compares the oligomerization of WT p53 with that of segments of p53. In the absence of glutaraldehyde, WT p53 electrophoresed as a monomer in the SDS-polyacrylamide gel. In the presence of 0.001% glutaraldehyde, p53 tetramers were only partially cross-linked and, therefore, were partially dissociated during SDS-PAGE. Monomers, dimers, trimers, and tetramers were evident under these conditions. At higher glutaraldehyde concentrations, preformed oligomers were fully cross-linked and were not dissociated by the SDS-polyacrylamide gel buffer at all. Because intramolecular cross-linking results in a more compact and less flexible molecular structure, increasing glutaraldehyde concentrations led to slightly more rapid electrophoretic mobilities for each oligomeric species. When fully cross-linked, WT p53 formed tetramers and multiples of tetramers. The complete absence of other oligomeric forms confirms that glutaraldehyde did not cause artifactual intermolecular cross-linking. Segments 280–390 and 315–360 formed tetramers but not multiples of tetramers.

Cross-linking of segment 1–320 did not demonstrate any oligomerization at low concentrations of glutaraldehyde. Retardation of this segment to the top of the gel at higher glutaraldehyde concentrations, however, suggests that segment 1–320 has a tendency to aggregate. Segments 80–320 and 330–390 formed mostly monomers under our experimental conditions regardless of the concentration of glutaraldehyde used to cross-link preparations. Migration of these segments during SDS-PAGE increased with increasing glutaraldehyde concentrations. This finding confirms that the cross-linking reactions were successful and that they resulted in a more compact intramolecular structure but not in intermolecular cross-linking. We conclude that p53 segments 1–320, 80–320, and 330–390 do not form stable tetramers under the conditions that favor efficient tetramerization of WT p53 and of segments 280–390 and 315–360.

Oligomerization of murine segment 80–320 at increased protein concentrations. During gel filtration, a small portion of segments 1–320 and 80–320 eluted as indistinct leading shoulders ahead of the predominant monomer peaks. This finding suggested to us that these segments may form transient oligomeric forms. Figure 5 shows further analyses of segment 80–320 at a protein concentration four times that used in Fig. 3. Under these conditions, gel filtration (Fig. 5A) revealed a more prominent leading shoulder in the elution profile of segment 80–320 but not those of other segments included as internal markers. Ahead of the major monomer peak, there was a less distinct peak at the expected position of dimers. In addition, the segment eluted well ahead of the apparent dimer peak, even though no distinct peaks were evident at these positions. Furthermore, cross-linking of segment 80–320 and

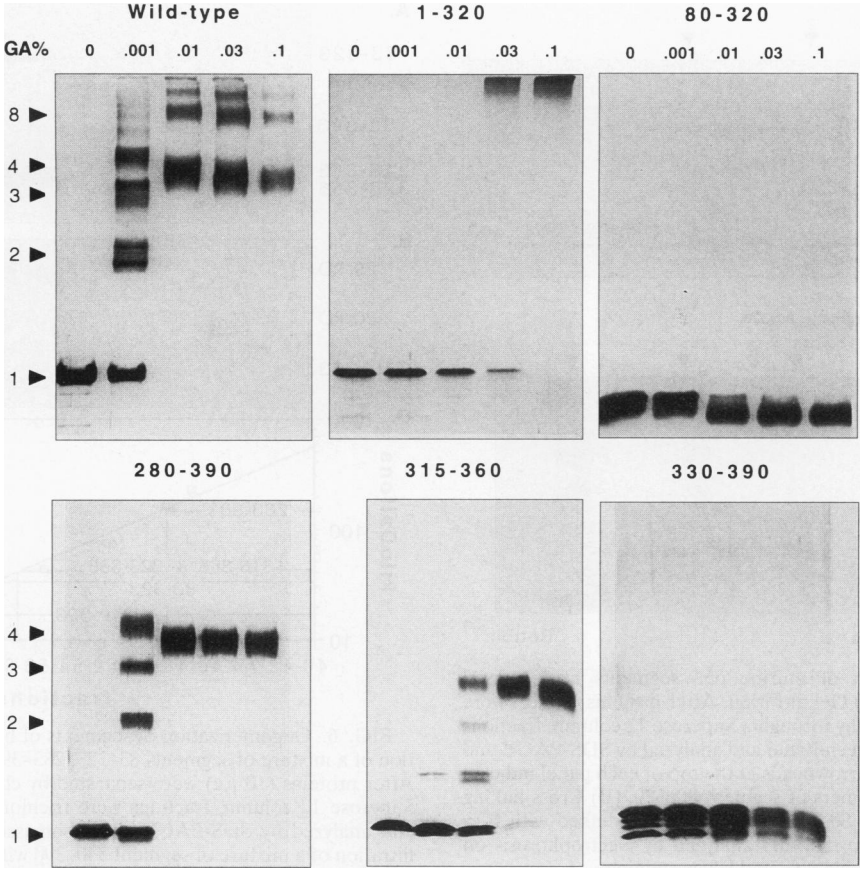

FIG. 4. Analysis of murine p53 quaternary structure by protein cross-linking and SDS-PAGE. Purified WT p53 and segments of p53 (2 μg) were cross-linked with 0 to 0.1% glutaraldehyde (GA%) for 30 min and analyzed by electrophoresis on SDS–4 to 20% or 8 to 20% polyacrylamide gels and silver staining. Molecular mass markers were analyzed in parallel but are not shown. Arrowheads indicate expected positions of oligomers.

analysis by SDS-PAGE at higher protein concentrations (Fig. 5B) demonstrated a continuous ladder of oligomeric forms under conditions of complete cross-linking. Thus, both assays show that segment 80–320 has the potential to form weak oligomers without an obvious preference for any particular form and that this oligomerization is related to protein concentration. Figure 5A also shows that murine segment 315–350 behaves like tetramers during gel filtration.

Gel filtration of human p53 segments. Having characterized the oligomerization properties of segments of murine p53, we cloned, expressed, and purified equivalent segments of human p53 for comparative analyses. Figure 6 shows properties of several human p53 segments during gel filtration. Standard markers run under the same conditions are not shown but are plotted in Fig. 6C. Most of human segment 83–323 eluted from the column between ovalbumin (45 kDa) and carbonic anhydrase (29 kDa) at the expected position of a globular monomer. As in the case of its murine counterpart, this segment eluted with a small leading shoulder, suggesting that it also forms unstable oligomers that dissociate during analysis. Human segment 283–393, like murine p53 segment 280–390 shown in Fig. 3, had an apparent mass greater than 100 kDa. Human segments 318–363 and 323–355 eluted one to two fractions ahead of the larger segment 83–323 at the position expected for tetramers. Figure 6B compares the elution profile of human segment 340–393 with those of carbonic anhydrase (29 kDa) and soybean trypsin inhibitor (20 kDa) added as internal markers in the same gel filtration column. Segment 340–393 eluted one to two fractions behind the 20-kDa internal marker. We conclude that segment 340–393, whose SDS-polyacrylamide gel molecular mass is 13 kDa, does not form stable tetramers. Cross-linking and SDS-PAGE confirmed that segment 340–393 consists mostly of monomers (data not shown). Comparison of Fig. 6 with Fig. 3 indicates that equivalent human and murine segments behave remarkably similarly during gel filtration.

Transformation by murine p53 segments. We have previously studied the ability of p53 segments to enhance transformation by the oncogenes *ras* and E1A (22). In those studies, however, p53 segments were expressed under the control of the relatively weak Moloney sarcoma virus promoter and we could not quantitate the expression levels of p53 segments. Here, we have used the strong cytomegalovirus immediate-early promoter to enhance p53 expression. Figure 7A shows representative results based on three independent experiments. Primary REF cells were cotransfected with plasmids expressing *ras*, E1A, and a control plasmid to establish a baseline level of transformation by *ras* and E1A (Fig. 7A). Cotransfection of WT p53 with *ras* and E1A significantly suppressed transformation as previously reported (22). Segment 1–320 also suppressed transformation but to a more limited extent than did WT p53. Our previous results with a weak promoter for p53 expression showed that segment 1–320 had no significant suppression function (22). Segment 1–320,

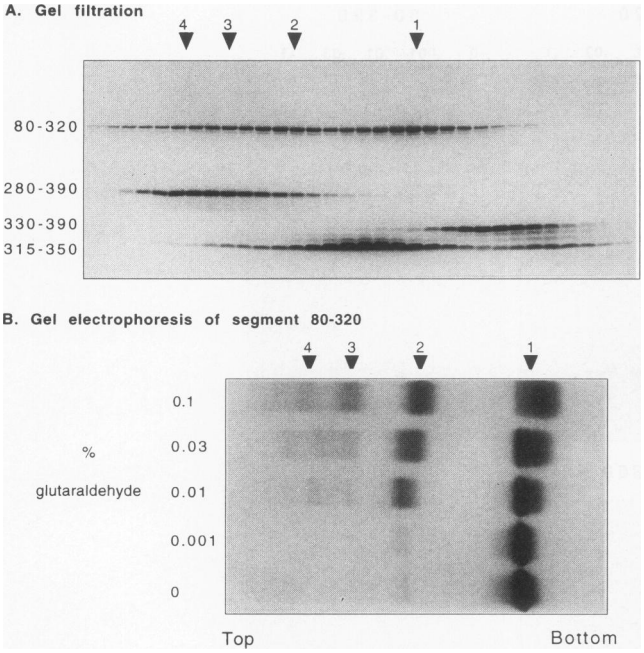

FIG. 5. Oligomerization of murine p53 segments at increased protein concentrations. (A) Gel filtration. After proteins (40 μg) were separated by chromatography through a Superose 12 column, fractions were trichloroacetic acid precipitated and analyzed by SDS-PAGE and Coomassie blue staining. Arrowheads at the top of each panel indicate expected positions of oligomers of segment 80–320. (B) Cross-linking and SDS-PAGE. Segment 80–320 (8 μg) was cross-linked with 0 to 0.1% glutaraldehyde for 30 min and analyzed by electrophoresis on SDS–8 to 20% polyacrylamide gels and silver staining.

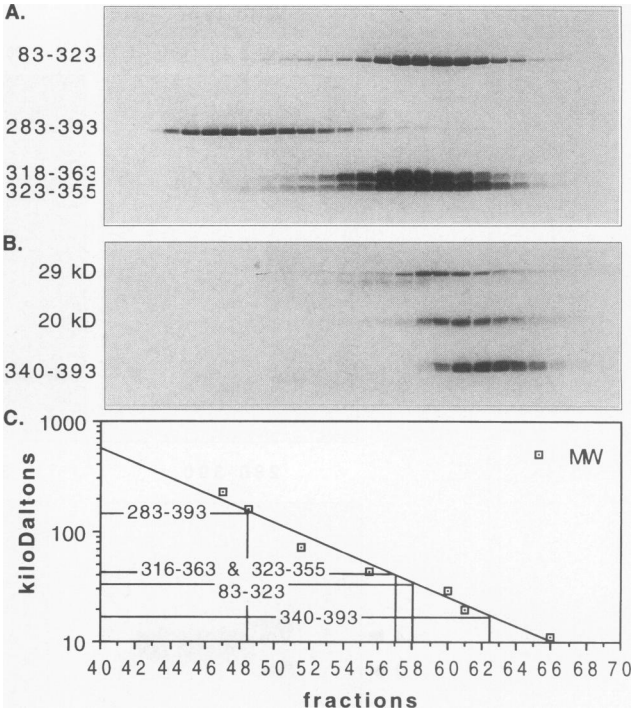

FIG. 6. Oligomerization of segments of human p53. (A) Gel filtration of a mixture of segments 83–323, 283–393, 318–363, and 323–355. After proteins (10 μg) were separated by chromatography through a Superose 12 column, fractions were trichloroacetic acid precipitated and analyzed by SDS-PAGE and Coomassie blue staining. (B) Gel filtration of a mixture of segment 340–390 with carbonic anhydrase (29 kDa) and soybean trypsin inhibitor (20 kDa). (C) Molecular mass plot of standard markers. The positions of p53 segments are related to their apparent molecular masses by horizontal and vertical lines.

therefore, has partial suppression activity but only when expressed at high levels. Segment 80–320 had no significant effect on transformation by *ras* and E1A in either study. In contrast, segments 280–390 and 315–360 enhanced transformation significantly. Finally, segment 330–390 had no apparent effect on transformation. We conclude that the ability of p53 segments 280–390 and 315–360 to tetramerize correlates very well with their ability to enhance transformation by other oncogenes. We cannot completely exclude the possibility that segments 280–390 and 315–360 have autonomous positive transforming activities.

We compared the levels of protein expression in REF cells transfected by plasmids expressing the same segments used in the transformation studies described above. We used a combination of metal affinity precipitation and immunoblotting techniques to quantitate the levels of accumulated p53 (Fig. 7B). With the exception of segment 315–350 (data not shown) and segment 330–390, p53 segments accumulated at significant levels. Although segment 280–390 accumulated to very high levels, it did not transform more efficiently than segment 315–360 did. We conclude that the levels of segment 315–360 are probably sufficient to saturate and inactivate the suppression activity of endogenous p53. With the exception of segments 315–350 and 330–390, therefore, the remaining segments were probably expressed at levels sufficient to demonstrate their intrinsic functions. The lack of accumulation of segments 315–350 and 330–390 in animal cells precludes meaningful interpretation of the role of these segments in transformation.

DISCUSSION

We have analyzed the structural properties of purified WT p53 and segments of p53 by a variety of approaches. In agreement with others (8), we find that WT p53 appears to have a nonglobular shape. We have shown here that the C terminus is the major determinant of that shape. Interestingly, we find that murine p53 has two autonomous oligomerization domains. Segments 280–390, 315–360, and 315–350 form stable tetramers. Segments 1–320 and 80–320 form transient oligomers without apparent preference for specific oligomeric forms. We hereafter refer to oligomerization by the two domains as tetramerization and nontetrameric oligomerization to indicate the differences in the domains. Finally, our studies show that corresponding segments of murine and human p53 have similar properties.

Contribution of p53 domains to the apparent nonglobular shape of p53. Protein cross-linking in conjunction with SDS-PAGE indicates that purified WT p53 consists predominantly of tetramers and to a lesser extent of multiples of tetramers. After gel filtration, however, WT p53 elutes at a position that corresponds to a mass significantly larger than that of a globular tetramer. These results are very similar to those of Friedman et al. (8) and support the idea that p53 has a nonglobular shape. After gel filtration, segment 1–320 eluted somewhat ahead of the position one would expect if it were a monomer. Perhaps this behavior is related to its aberrant behavior during SDS-PAGE. Segment 80–320 behaves predominantly as a monomer during gel filtration and, therefore,

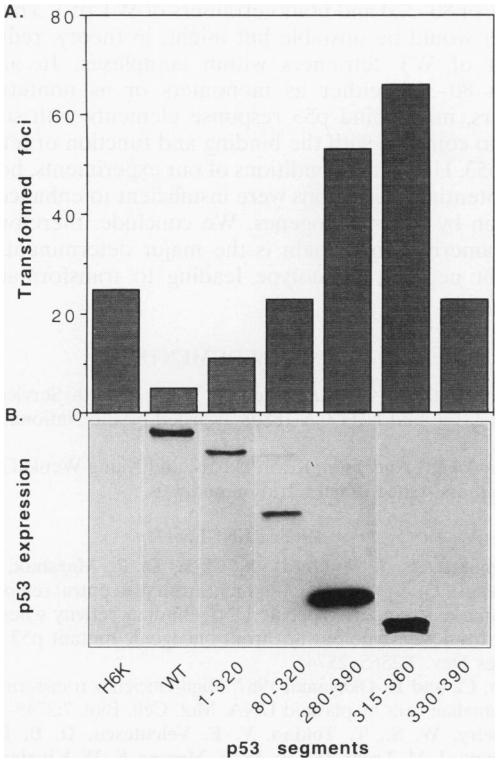

FIG. 7. Suppression and transformation by murine WT p53 and segments of p53. (A) Histogram of transformed colonies. REF cells were cotransfected with plasmids expressing adenovirus E1A and *ras* to establish a baseline of transformation. The effects of cotransfection of a control plasmid or plasmids expressing p53 on transformation are shown in the histogram. (B) Accumulation of p53. REF cells were transfected with plasmids expressing WT p53 or segments of p53. The tagged p53s were concentrated by metal affinity selection and analyzed by immunoblotting with monoclonal antibodies against the hemagglutinin tag as described in Materials and Methods.

does not contribute significantly to the anomalous behavior of WT p53. In contrast, the largest C-terminal segment, consisting of amino acids 280 to 390, behaved quite anomalously during gel filtration even when its quaternary structure was taken into account. Segment 280–390 would have a molecular mass of 60 kDa as a tetramer but eluted from gel filtration columns at the position of a globular mass of well over 100 kDa. These findings could mean that WT p53 and segment 280–390 form octomers, but tetramers were the predominant forms evident by cross-linking analyses. Alternatively, WT p53 and segment 280–390 could possibly assume larger masses by binding to nucleic acids contaminating our preparations of purified p53. DNase and RNase treatments had no effect on the gel filtration of WT p53 or segment 80–320, and no DNA or RNA contamination was evident in our preparations by electron microscopy (data not shown). Our findings, therefore, argue that the intrinsic structure of WT p53 and segment 280–390 is nonglobular.

Because both WT p53 and segment 280–390 form stable tetramers, our findings suggest that tetramerization may contribute to the nonglobular shape of WT p53. The minimal tetramerization domain, however, is not sufficient to account for the apparent nonglobular shape of p53; tetramers of segments 315–360 and 315–350 demonstrate no significant anomalies during gel filtration. Tetramerization, therefore, may be necessary but not sufficient to account for the contribution of the C terminus to the unusual shape of p53.

The tetramerization domain. Murine p53 segments 280–390, 315–360, and 315–350 assemble stable tetramers. When fully cross-linked, only tetramers are evident as judged by gel electrophoresis. Because the same segments form tight symmetrical peaks during gel filtration in the absence of cross-linking, differences in the amount of glutaraldehyde required for complete cross-linking of these three segments probably reflect the availability of free amino groups for cross-linking rather than the stability of the tetramers. Wide ranges in pHs and ionic concentrations do not dissociate the tetramers, nor do chelating agents, reducing reagents, or nonionic detergents have a significant effect on the tetramers (data not shown). Our findings are in good agreement with those of Pavletich et al. (20), who showed recently that a proteolytic fragment of human p53 consisting of amino acids 311 to 365 forms stable tetramers, and with those of Halazonetis and Kandil (10), who presented evidence that murine segment 1–360 forms tetramers. Because murine amino acids 320 to 350 (human amino acids 323 to 355) are highly conserved in p53s from all species identified to date (22), we propose that this region represents the core tetramerization domain.

We were unable to detect significant oligomerization by murine segment 330–390 or human p53 segment 340–393 under our conditions. These findings differ from those of Sturzbecher et al. (28), who reported that human segment 340–393 forms tetramers. Their evidence for oligomerization was based on analysis by gel filtration and SDS-PAGE of cross-linked proteins, two of the assays that we used. They reported that human segment 340–393 elutes ahead of soybean trypsin inhibitor during gel filtration. In contrast, we found that segment 340–393 elutes behind soybean trypsin inhibitor used as an internal marker in our gel filtration column. Because of these differences, we sequenced the DNA encoding our C-terminal segments and found no errors in our constructions. Furthermore, the apparent masses of segments 330–390 and 340–393 analyzed by SDS-PAGE argue that these segments were not significantly digested by proteinase during preparation. We cannot account for the differences between our findings and those of Sturzbecher et al. Perhaps segment 340–393, which overlaps the tetramerization domain in segment 323–355, has weak oligomerization properties under other conditions. A side-by-side comparison, however, indicates that segment 315–350 forms tetramers efficiently while segment 340–393 consists mostly of monomers.

The function of the tetramerization domain is not clear. It is not absolutely required for site-specific DNA binding in vitro or for transactivation in vivo (1, 20, 29). It may, however, contribute to the suppression of transformation by other oncogenes. When expressed under the control of the relatively weak Moloney sarcoma virus promoter, segment 1–320 fails to suppress transformation by other oncogenes to any significant extent (22). In contrast, when expressed under the control of a strong cytomegalovirus promoter, segment 1–320 partially suppresses transformation. These findings are consistent with those of Shaulian et al. (24) and Slingerland et al. (25), who have shown that mutations within the tetramerization domain reduce suppression by p53 in a dose-dependent manner. In contrast, the tetramerization domain is both necessary and sufficient for the enhancement of transformation by other oncogenes. This finding supports the idea that the dominant negative phenotype of mutant p53s could be explained by the formation of mixed tetramers consisting of WT and mutant subunits. Nevertheless, the primary molecular function of tetramerization remains unclear. The strong tetramerization

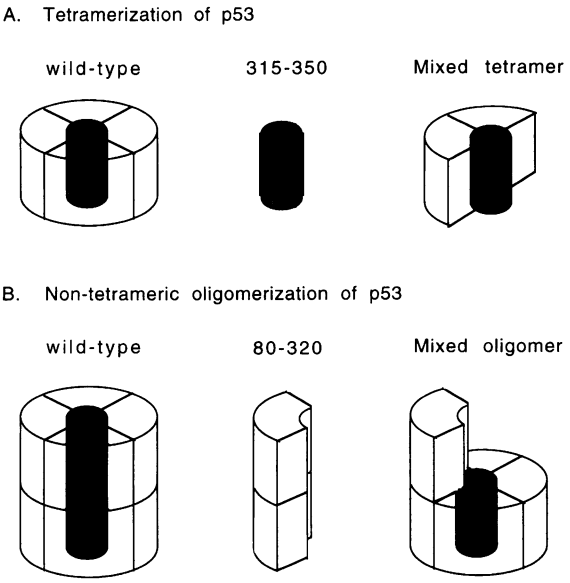

FIG. 8. Model for the oligomerization of p53. (A) Tetramerization by p53 and segment 315–360. (B) Nontetrameric oligomerization by WT p53 and segment 80–320.

domain, consisting of amino acids 315 to 350, is a part of p53 segment 315–390 that is capable of autonomous nonspecific DNA binding (29). The biological function of nonspecific DNA binding by p53, however, remains to be determined.

Nontetrameric oligomerization. Amino acids 80 to 320 represent a second autonomous oligomerization domain that is weak relative to the tetramerization domain within segment 315–350. The existence of this oligomerization domain in segment 80–320 has not been previously reported. We call this domain the nontetrameric oligomerization domain. One potential role for this oligomerization domain is apparent from its location. It is associated with the same p53 segment that is capable of specific binding to a p53 response element consisting of repeated sequences (1, 20, 29). Indeed, we have direct evidence by scanning transmission electron microscopy that multiple subunits of segment 80–320 bind to the DNA consensus sequence for specific binding by p53 (26a). This interaction leads to transactivation in vivo when the consensus DNA site is part of a model promoter (29).

Model for p53 oligomerization functions. Figure 8 summarizes the role of p53 domains in oligomerization. WT p53 forms two kinds of oligomers: tetramers and multiples of tetramers. In the figure, tetramers are shown as flat structures to represent their apparently nonglobular shapes. Isolated segments of p53 demonstrate two kinds of oligomerization. Segment 315–360, shown in gray in the figure, forms stable tetramers in a solution. Segment 1–320 forms mostly monomers in a solution but forms unstable oligomers under appropriate conditions. Taken together, these interactions would account for the formation of tetramers and multiples of tetramers by WT p53. Both isolated segments could also form mixed oligomers with WT p53 during intracellular synthesis. Segment 315–360 could form mixed tetramers with WT p53. Because these mixed oligomers would be stable and also deficient in transactivating functions, they would reduce the suppression function of endogenous WT p53 in cells and enhance transformation by other oncogenes. Segment 80–320 could form a different kind of mixed oligomer consisting of subunits of 80–320 and homotetramers of WT p53. This mixed oligomer would be unstable but might, in theory, reduce the function of WT tetramers within complexes. In addition, segment 80–320, either as monomers or as nontetrameric oligomers, might bind p53 response elements with sufficient affinity to compete with the binding and function of tetramers of WT p53. Under the conditions of our experiments, however, these potential interactions were insufficient to enhance transformation by other oncogenes. We conclude, therefore, that the tetramerization domain is the major determinant of the dominant negative phenotype leading to transformation by mutant p53s.

ACKNOWLEDGMENTS

This investigation was supported by Public Health Service grants NIH CA-28146 and NIH CA-18808 awarded by the National Cancer Institute.

We thank Carl Anderson, Kevin Harris, and Xiang Wenkai for their advice and assistance in gel filtration analyses.

REFERENCES

1. **Bargonetti, J., J. Manfredi, X. Chen, D. R. Marshak, and C. Prives.** 1993. A proteolytic fragment from the central region of p53 has marked sequence-specific DNA-binding activity when generated from wild-type but not from oncogenic mutant p53 protein. Genes Dev. **7**:2565–2574.
2. **Chen, C., and H. Okayama.** 1987. High-efficiency transformation of mammalian cells by plasmid DNA. Mol. Cell. Biol. **7**:2745–2752.
3. **El-Deiry, W. S., T. Tokino, V. E. Velculescu, D. B. Levy, R. Parsons, J. M. Trent, D. Lin, W. E. Mercer, K. W. Kinzler, and B. Vogelstein.** 1993. WAF1, a potential mediator of p53 tumor suppression. Cell **75**:817–825.
4. **Eliyahu, D., D. Michalovitz, S. Eliyahu, O. Pinhasi-Kimhi, and M. Oren.** 1989. Wild-type p53 can inhibit oncogene-mediated focus formation. Proc. Natl. Acad. Sci. USA **86**:8763–8767.
5. **Farmer, G., J. Bargonetti, H. Zhu, P. Friedman, R. Prywes, and C. Prives.** 1992. Wild-type p53 activates transcription in vitro. Nature (London) **358**:83–86.
6. **Fields, S., and S. K. Jang.** 1990. Presence of a potent transcription activating sequence in the p53 protein. Science **249**:1046–1049.
7. **Finlay, C. A., P. W. Hinds, and A. J. Levine.** 1989. The p53 proto-oncogene can act as a suppressor of transformation. Cell **57**:1083–1093.
8. **Friedman, P. N., X. B. Chen, J. Bargonetti, and C. Prives.** 1993. The p53 protein is an unusually shaped tetramer that binds directly to DNA. Proc. Natl. Acad. Sci. USA **90**:3319–3323.
9. **Funk, W. D., D. T. Pak, R. H. Karas, W. E. Wright, and J. W. Shay.** 1992. A transcriptionally active DNA-binding site for human p53 protein complexes. Mol. Cell. Biol. **12**:2866–2871.
10. **Halazonetis, T. D., and A. N. Kandil.** 1993. Conformational shifts propagate from the oligomerization domain of p53 to its tetrameric DNA binding domain and restore DNA binding to select p53 mutants. EMBO J. **12**:5057–5064.
11. **Harper, J. W., G. R. Adami, N. Wei, K. Keyomarsi, and S. J. Elledge.** 1993. The p21 Cdk-interacting protein Cip1 is a potent inhibitor of G1 cyclin-dependent kinases. Cell **75**:805–816.
12. **Herskowitz, I.** 1987. Functional inactivation of genes by dominant negative mutations. Nature (London) **329**:219–222.
13. **Hinds, P., C. Finlay, and A. J. Levine.** 1989. Mutation is required to activate the p53 gene for cooperation with the *ras* oncogene and transformation. J. Virol. **63**:739–746.
14. **Hollstein, M., D. Sidransky, B. Vogelstein, and C. C. Harris.** 1991. p53 mutations in human cancers. Science **253**:49–53.
15. **Kern, S. E., J. A. Pietenpol, S. Thiagalingam, A. Seymour, K. W. Kinzler, and B. Vogelstein.** 1992. Oncogenic forms of p53 inhibit p53-regulated gene expression. Science **256**:827–830.
16. **Laemmli, U. K.** 1970. Cleavage of structural proteins during the assembly of the head of bacteriophage T4. Nature (London) **227**:680–685.
17. **Levine, A. J., J. Momand, and C. A. Finlay.** 1991. The p53 tumour suppressor gene. Nature (London) **351**:453–456.

18. **Milner, J., E. A. Medcalf, and A. C. Cook.** 1991. Tumor suppressor p53: analysis of wild-type and mutant p53 complexes. Mol. Cell. Biol. **11:**12–19.
19. **Oakley, B. R., D. R. Kirsch, and N. R. Morris.** 1980. A simplified ultrasensitive silver stain for detecting proteins in polyacrylamide gels. Anal. Biochem. **105:**361–363.
20. **Pavletich, N. P., K. A. Chambers, and C. O. Pabo.** 1993. The DNA-binding domain of p53 contains the four conserved regions and the major mutation hot spots. Genes Dev. **7:**2556–2564.
21. **Pennica, D., D. V. Goeddel, J. S. Hayflick, N. C. Reich, C. W. Anderson, and A. J. Levine.** 1984. The amino acid sequence of murine p53 determined from a c-DNA clone. Virology **134:**477–482.
22. **Reed, M., Y. Wang, G. Mayr, M. E. Anderson, J. F. Schwedes, and P. Tegtmeyer.** 1993. p53 domains: suppression, transformation, and transactivation. Gene Expression **3:**95–107.
23. **Shaulian, E., A. Zauberman, D. Ginsberg, and M. Oren.** 1992. Identification of a minimal transforming domain of p53: negative dominance through abrogation of sequence-specific DNA binding. Mol. Cell. Biol. **12:**5581–5592.
24. **Shaulian, E., A. Zauberman, J. Milner, E. A. Davies, and M. Oren.** 1993. Tight DNA binding and oligomerization are dispensable for the ability of p53 to transactivate target genes and suppress transformation. EMBO J. **12:**2789–2797.
25. **Slingerland, J. M., J. R. Jenkins, and S. Benchimol.** 1993. The transforming and suppressor functions of p53 alleles—effects of mutations that disrupt phosphorylation, oligomerization and nuclear translocation. EMBO J. **12:**1029–1037.
26. **Srinivasan, R., J. A. Roth, and S. A. Maxwell.** 1993. Sequence-specific interaction of a conformational domain of p53 with DNA. Cancer Res. **53:**5361–5364.

26a. **Stenger, J. E., et al.** Personal communication.

27. **Stenger, J. E., G. A. Mayr, K. Mann, and P. Tegtmeyer.** 1992. Formation of stable p53 homotetramers and multiples of tetramers. Mol. Carcinog. **5:**102–106.
28. **Sturzbecher, H.-W., R. Brain, C. Addison, K. Rudge, M. Remm, M. Grimaldi, E. Keenan, and J. R. Jenkins.** 1992. A C-terminal a-helix plus basic region motif is the primary structural determinant of p53 tetramerization. Oncogene **7:**1513–1523.
29. **Wang, Y., M. Reed, P. Wang, J. E. Stenger, G. Mayr, M. E. Anderson, J. F. Schwedes, and P. Tegtmeyer.** 1993. p53 domains: identification and characterization of two autonomous DNA-binding regions. Genes Dev. **7:**2575–2586.